Proceedings of the 21st ICSMGE, Vienna, Austria, 14 – 19 June 2026. Pistrol, Adam & Schweiger (eds.)
Published by: ÖGG, Austrian Society for Geomechanics, Salzburg, Austria, ISBN 978-3-9503898-4-5
https://doi.org/10.53243/ICSMGE2026-2321

Hybrid ground response simulation and effective stress analysis considering steady state of sand

Tomoya Onodera, Ryuichi Ibuki, Jun Izawa
Railway Technical Research Institute, Tokyo, Japan, onodera.tomoya.06@rtri.or.jp

Kiyoshi Fukutake
Ohsaki Research Institute, Tokyo, Japan

Takatoshi Kiriyama
Shimizu Corporation, Tokyo, Japan

ABSTRACT: This study first discusses the steady state behavior that occurs during large ground deformations. The authors propose an improved effective stress analysis model, termed the "extended bowl model," by modifying the original bowl model to incorporate the steady state behavior. In this model, when the soil reaches a critical void ratio, further increases in void ratio are prevented. Under undrained conditions, the model captures the limitation in the increment of effective stress, enabling more accurate simulation of the behavior of liquefiable soils under large deformation. To validate the proposed model, a series of hybrid ground response simulations using Toyoura sand were conducted to experimentally evaluate ground behavior during extremely large earthquakes. This test integrates a physical soil specimen into numerical analysis through dynamic response feedback, providing a highly accurate representation of ground behavior. Reproduction analyses using the extended bowl model combined with the GHE model was then performed. In the tests, the target layer reached a steady state under input seismic motions exceeding 5,000 Gal. While the original bowl model overestimated the effective stress and acceleration of the surface ground, the extended bowl model successfully reproduced the peak effective stress. Consequently, the calculated ground response, such as acceleration and deformation, under extremely large input seismic motions showed good agreement with the experimental data. The results demonstrate the necessity of accounting for steady state behavior when modeling sandy soils and suggest that the proposed model provides a reliable analytical method for evaluating seismic ground response under extremely large earthquake motions.

KEYWORDS: liquefaction, effective stress analysis, steady state, hybrid ground response simulation

1 INTRODUCTION

In the Japanese Design Standard for Railway Structures, the Level 2 design seismic motion is defined as the maximum possible ground motion that may occur at the construction site. It is recommended that this seismic motion for the design be calculated using a strong-motion prediction method, which takes into account of fault models or site-specific conditions. In recent years, concerns have arisen regarding the potential occurrence of extremely large earthquakes, such as the Nankai Trough Earthquake, with magnitudes exceeding 9, and the possibility of strong ground motions occurring near the epicenter. In order to assess the seismic performance of structures, it is first necessary to evaluate the seismic behavior of surface ground, including soil liquefaction phenomena using an effective stress analysis model of soil, which considers the effect of excess pore water pressure. In particular, when considering such extremely large-scale earthquakes, it is essential to account for a "steady state," a condition in which the soil undergoes continuous shear deformation without further increase in effective stress and shear stress.

For nonlinear total stress analysis of soils, the GHE-S model, a modified version of the GHE model, is commonly used in the seismic design of Japanese railway structures. The GHE-bowl model, which is the combination of the GHE model and the bowl model, has been proposed as an effective stress model capable of capturing changes in excess pore water pressure. The "original" bowl model, however, cannot represent a steady state at a large strain level, resulting in inaccurate predictions of the seismic ground response under extremely large earthquake conditions. In this study, we attempt to extend the original bowl model to incorporate a steady state behavior of liquefiable ground and propose a parameter-setting method to achieve this. Finally, validity of the proposed model was confirmed through a series of reproducing analyses of hybrid ground-response simulations, which combine a simple shear laboratory testing with a numerical ground response analysis.

2 STEADY STATE AND EXTENDED BOWL MODEL

2.1 *Steady state of sandy soils*

Yoshimine and Ishihara (1998) introduced the concept of a steady state of sandy soils. Fig. 1 shows conceptual diagrams of soil deformation behavior under monotonic shear loading. The steady state is generally defined as a phenomenon at which shear strain increases without any further increase of effective stress at large strain level under undrained conditions as shown in Fig.1(a). Under undrained conditions, the effective stress of loose sand decreases during shearing and reaches a steady state with a lower effective stress, $\sigma'_{s,3}$, than the initial effective stress, σ'_0. In contrast, dense sand exhibits an increase in effective stress, reaching a steady state with higher effective stress, $\sigma'_{s,1}$. Thus, when the initial effective stress is the same, the effective stress at the steady state depends on the initial void ratio, or the density. We refer to the effective stress at the steady state as the "critical steady state," σ'_s.

In contrast, under drained conditions, the void ratio of the soil converges to a constant value at large strain level, regardless of the initial void ratio, as shown in Fig. 1(b). We refer to this converged void ratio as the "critical void ratio," e_{cr}. This drained behavior is also referred to as a steady state and regarded as an equivalent phenomenon to the undrained one in this study. We aim to incorporate this phenomenon into the bowl model, which can calculate change in volumetric strain with change in shear strain, as explained in the next chapter.

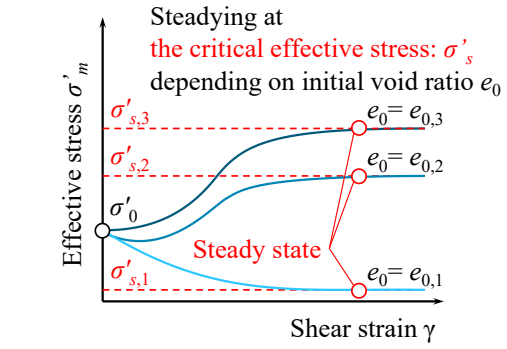

(a) Undrained condition

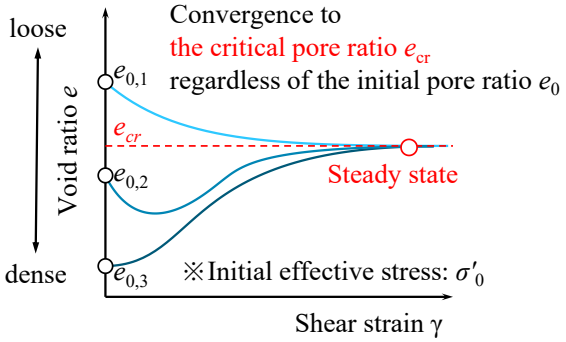

(b) Drained condition

Figure 1. Conceptual figure of soil deformation under simple shearing

2.2 *Extended bowl model*

The bowl model proposed by Fukutake and Matsuoka (1989) and later verified by, for example, Fukutake and Kiriyama (2018), calculates the volume change due to shearing under drained conditions by separating it into two components: resultant shear strain Γ and cumulative shear strain G^*, as illustrated in Fig. 2, which presents the conceptual volume change considered in the original bowl model. The cumulative shear strain causes volumetric compression, as described by Equation (1), and the resultant shear strain leads to volumetric swelling, as described by Equation (2).

$$\varepsilon^c = \frac{G^*}{C + DG^*} \tag{1}$$

$$\varepsilon^s = A\Gamma^B \tag{2}$$

Here, A, B, C, and D are the parameters for the bowl model respectively. The original bowl model explains the volumetric changes caused by shearing, dilatancy, by combining those two components. It should be noted that the definitions of Γ and G^* used here are based on Equation (3), as applied in the authors' one-dimensional effective stress analysis, and are adapted from the three-dimensional formulation developed in previous studies.

$$\Gamma = \gamma \tag{3a}$$

$$G^* = \Sigma|\Delta\gamma| \tag{3b}$$

In order to simulate the behavior under undrained conditions, dilatancy $d\varepsilon_v^s$ is converted into an increment in the effective mean stress $d\sigma'_m$ using Equation (4), which explains that the volume change through shear loading is zero.

$$d\sigma'_m = \frac{\sigma'_m \cdot d\varepsilon_v^s}{0.434(C_s or C_s')/(1+e_0)} \tag{4}$$

Here, C_s and C_s' are the calibration parameters used to control shear strain development under undrained cyclic shear conditions; they are empirically determined and not derived from compression test results.

However, this model does not account for the maximum values of the volume, or void ratio, because the swelling component ε^s which is calculated by the power of Γ continues to increase indefinitely in the large strain level, resulting in an unbounded increase of the void ratio. In the case of undrained shearing, this limitless increase in effective stress can lead to an overestimation of shear stress and acceleration response.

To address this problem, we proposed the extended bowl model, which modifies the original bowl model to incorporate steady state behavior by imposing a limit on the void ratio under drained conditions, or on the effective stress under undrained conditions. First, the model was formulated under drained conditions. In the extended bowl model, the "bowl" translates in parallel once the soil reaches a critical void ratio, beyond which no further increase in void ratio occurs, as illustrated in Fig. 3. Specifically, a critical resultant shear strain Γ_{f0} is defined as the resultant strain at which the soil enters the steady state. Once Γ reaches Γ_{f0}, the void ratio remains constant until unloading occurs. Additionally, during this phase, the updating of the cumulative shear strain G^* is suspended. In cyclic shear loading, this mechanism is applied repeatedly. Under undrained conditions, the steady state is characterized by a condition in which the increment of effective stress becomes zero, as shown in Fig. 1(b). This behavior is modeled by applying Equation (4), allowing the model to simulate the limitation of effective stress growth. Through this modification, the model prevents overestimation of shear stress and effective stress at large strain levels, resulting in more accurate predictions of the stress state. Consequently, the evaluation of the acceleration and displacement responses to extremely large earthquakes is expected to become more precise.

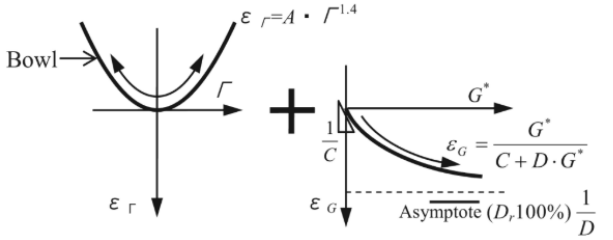

Figure 2. Concept of the original bowl model (Fukutake and Kiriyama, 2018)

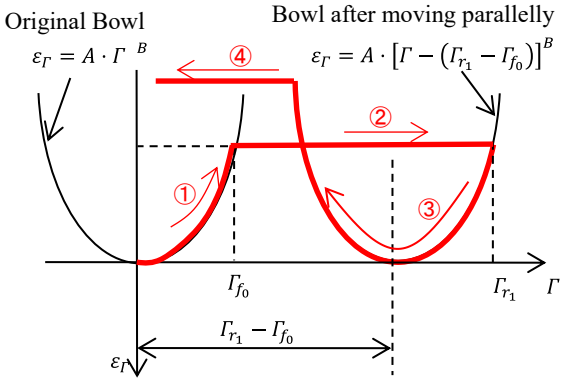

Figure 3. Concept of the extended bowl model

2.3 *Parameter setting*

In this study, Toyoura sand (with a relative density, D_r=60%) was used as the target layer in the hybrid ground response test for validation of the extended bowl model, as described in detail in Chapter 3. This section explains the procedure for setting the parameters of the extended bowl model.

Before setting the parameters for the extended bowl model, the physical parameters such as shear strength and deformation properties were determined for the total stress analysis. First, the internal friction angle ϕ' and the effective stress at the steady state σ_s' were obtained from the undrained monotonic shear test, as shown in Fig. 4.

Second, the GHE parameters were set using $G\sim\gamma$ and $h\sim\gamma$ relationships obtained from cyclic shear tests. The skeleton curve of the GHE model is represented by the generalized hyperbolic equation, given in Equation (5), where τ denotes the shear stress, τ_f the shear strength, γ the shear strain.

$$\tau/\tau_f = \frac{\gamma/\gamma_r}{\frac{1}{C_1(\gamma/\gamma_r)} + \frac{\gamma/\gamma_r}{C_2(\gamma/\gamma_r)}} \tag{5}$$

The reference shear strain γ_r is defined by Equation (6), using τ_f and the initial shear stiffness G_0. The GHE model consists of six parameters: $C_1(0)$, $C_1(\infty)$, $C_2(0)$, $C_2(\infty)$, α, and β, which are defined by Equation (7) and (8). Further details on the GHE model can be found in Tatsuoka and Shibuya (1992) and Nogami et al. (2012).

$$\gamma_r = \tau_f/G_0 \tag{6}$$

$$C_1(\gamma/\gamma_r) = \frac{C_1(0)+C_1(\infty)}{2} + \frac{C_1(0)-C_1(\infty)}{2}\cdot\cos\left\{\frac{\pi}{\alpha(\gamma/\gamma_r)+1}\right\} \tag{7}$$

$$C_2(\gamma/\gamma_r) = \frac{C_2(0)+C_2(\infty)}{2} + \frac{C_2(0)-C_2(\infty)}{2}\cdot\cos\left\{\frac{\pi}{\beta(\gamma/\gamma_r)+1}\right\} \tag{8}$$

It should be noted that both tests were conducted using a hollow cylindrical torsional shear test apparatus. Since the $G\sim\gamma$ relationship obtained from the test reflects the increase in excess pore water pressure due to cyclic loading, a modified shear stiffness G_{mod} was determined as shown in Equation (9), in order to exclude the effect of the excess pore water pressure, which is taken into account by the bowl model. This assumes that shear stiffness is proportional to the square root of the effective stress, as described in Equation (9). By comparing the $\tau\sim\gamma$ and $G\sim\gamma$ relationships before and after this modification, it was found that the influence of excess pore water pressure begins to appear at approximately 0.1% shear strain in the case of Toyoura sand, as shown in Figs. 5 and 6. By fitting to this modified test results as shown in Fig. 5, the GHE parameters were set. As illustrated in Fig. 6, the GHE model closely matches the $G/G_0\sim\gamma$ and $h\sim\gamma$ relationships obtained from the cyclic shear test. The deformation characteristics of Toyoura sand are well captured by the GHE model.

$$G_{mod} = G_{test}\left(1-\frac{\Delta u}{\sigma_{m0}'}\right)^{0.5} \tag{9}$$

Subsequently, the bowl model parameters are set by fitting to the relationship between cyclic shear stress ratio τ/σ_{m0}' and number of cycles N_c obtained from the liquefaction test: a series of undrained cyclic shear tests, as shown in Fig. 7. The parameter fitting was performed through trial and error by repeatedly conducting element simulations until a satisfactory match with the test results was achieved.

Table 1 shows the parameters for Toyoura sand (with D_r=60%). G_0 and γ_r are the initial shear stiffness and the reference shear strain at the confining pressure of the target layer, while those values are affected by the condition of confining pressure. In order to consider the steady state in the extended bowl model, $\sigma_s' = 320$kPa was used as a parameter based on the results of the monotonic shear test. When the effective stress reaches 320kPa in the calculation, the increment of the effective stress becomes zero, resulting in the shear stress and acceleration response reaching a plateau.

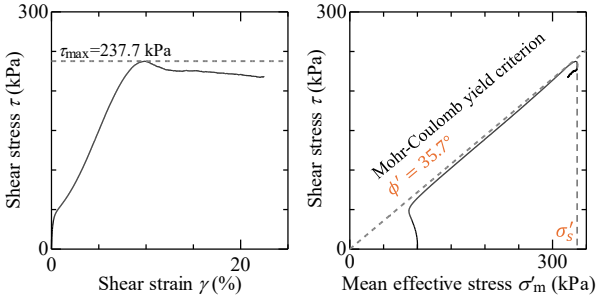

(a) $\tau\sim\gamma$ relationships (b) Effective stress path

Figure 4. Results of the undrained monotonic shear test

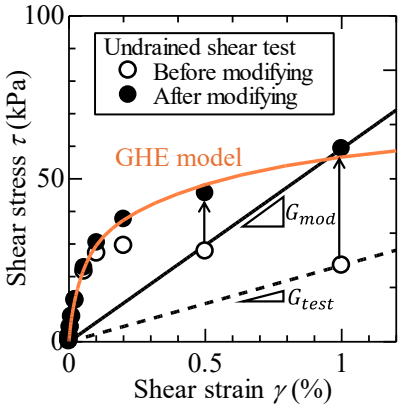

Figure 5. Fitting for the deformation property test results

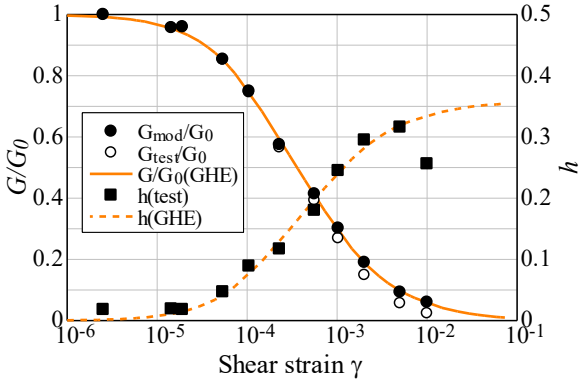

Figure 6. Fitting for the $G/G_0\sim\gamma$ and $h\sim\gamma$ relationships

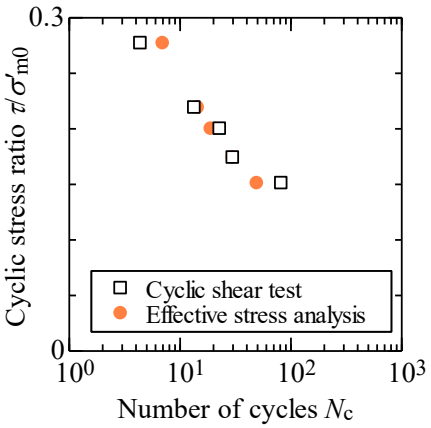

Figure 7. Fitting for the liquefaction test results

Table 1. Parameters of Toyoura sand D_r=60%

(a) Physical parameters of Toyoura sand

G_0(kPa)	γ_r(%)	ϕ' (°)	c (kPa)
4.39×10^4	3.27×10^{-2}	35.7	0.0

(b) GHE model parameters

$C_1(0)$	$C_1(\infty)$	$C_2(0)$	$C_2(\infty)$	α	β	h_{max}	κ
1.00	0.265	0.424	1.00	1.32	0.97	0.36	1.1

(c) Bowl model parameters

A	B	C	D	$C_s'/(1+e_0)$	$C_s'/(1+e_0)$	X_l	σ_s'
-0.5	1.4	10	30	0.01	0.0102	0.15	320kPa

3 VERIFICATION BY REPRODUCTION ANALYSIS

3.1 *Hybrid ground response test*

A hybrid ground response test was conducted to obtain accurate ground response for validating the extended bowl model. The apparatus and the conceptual diagram of the hybrid ground response test are shown in Fig. 8 and Fig. 9, respectively. In this test, the target layer in a ground response analysis is replaced with a soil specimen used in a simple shear test under confining pressure. The specimen is cylindrical with 20 mm in height and 60 mm in diameter, and is surrounded by a series of stacked rings. The reaction force of the target layer can be obtained from the soil specimen without mathematical modeling, by applying a seismic displacement data obtained in the previous step of the response analysis. This reaction force is then fed back into the next step of the response analysis. As a result, this test provides highly accurate response of the target layer, eliminating errors from numerical modeling and parameter-setting, even when the target layer consists of liquefiable soils.

Fig. 10 shows the model ground used in this study. In this model, the sand layer at a depth of 4~6 m was replaced by the simple shear test for Toyoura sand with D_r=60%. The seismic motion specified in the seismic design standard for Japanese railway structures was applied to the base layer (V_s=400m/sec, ρ=2.0g/cm^3) with maximum amplitudes scaled to 3,000, 5,000, and 7,000 Gal in order to investigate the ground responses under extremely large earthquakes. Rayleigh damping was applied to the model, with α=3.78, β=4.53×10^{-4}.

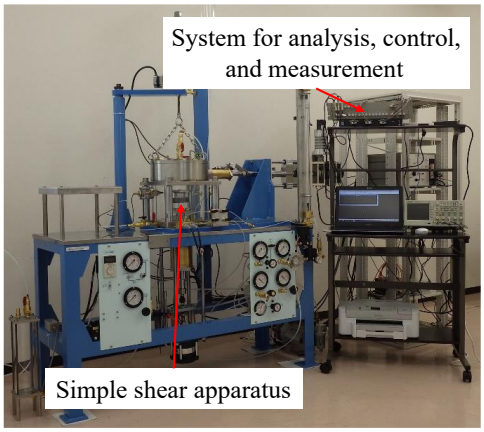

Figure 8. Hybrid ground response test apparatus

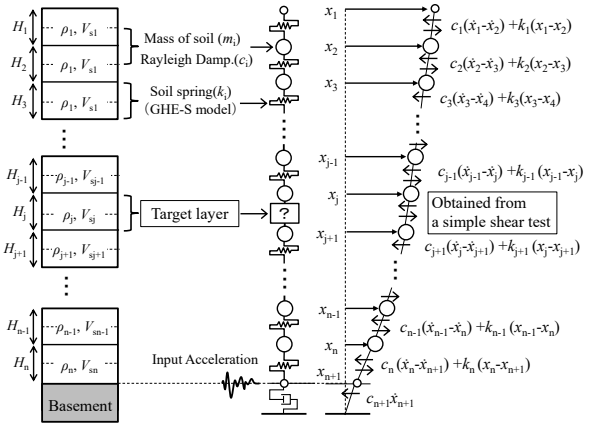

Figure 9. Conceptual figure of hybrid ground response test (Izawa et al., 2019)

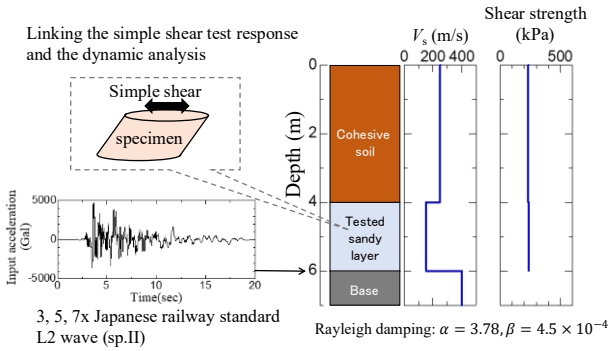

Figure 10. Target layer model and input earthquake waves

3.2 *Reproduction analysis by the extended bowl model*

A series of reproduction analyses of the hybrid ground response tests were conducted using the original bowl model and the extended bowl model. The results were compared with the experimental data to validate the extended bowl model.

Fig. 11 shows the vertical distribution of shear stress, horizontal displacement, and horizontal acceleration obtained from the hybrid ground response test and the effective stress analysis. When the input motion had a peak acceleration of 3,000 Gal, there was no significant difference between the original and the extended bowl model; both showed good agreement with the test results.

On the other hand, for input motion of 5,000 and 7,000 Gal, notable differences were observed in the behavior of the test

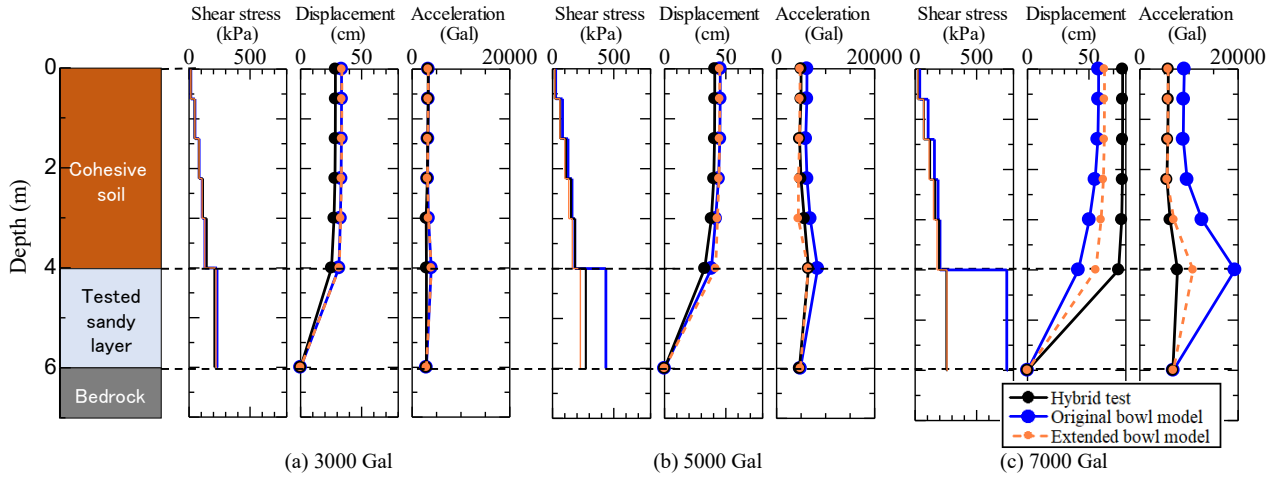

Figure 11. Depth distribution of maximum responses

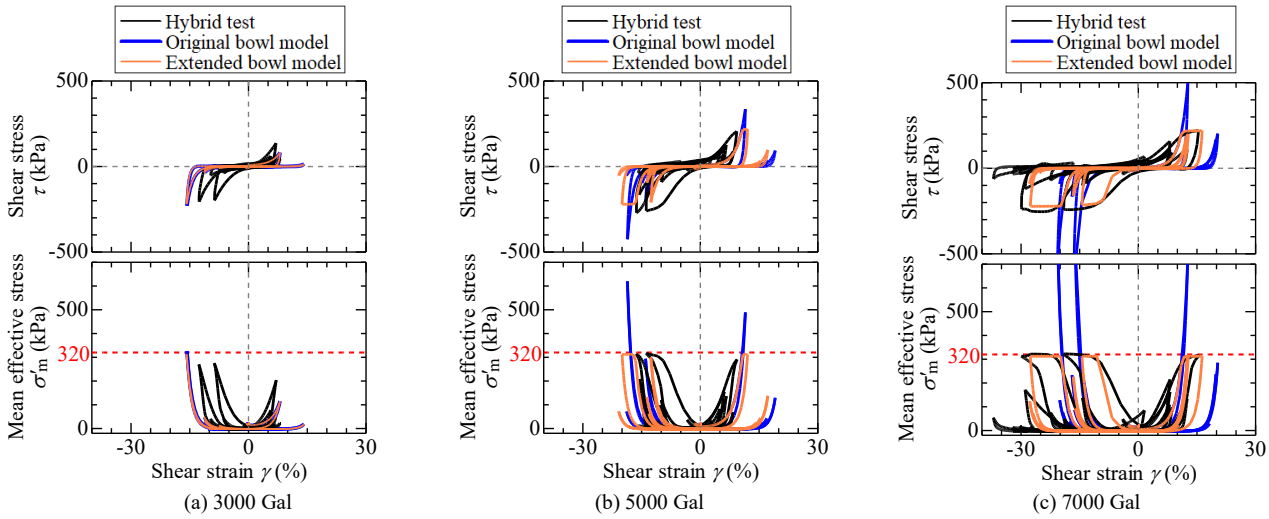

Figure 12. Hysteresis curves of the tested / effective stress analysis layer

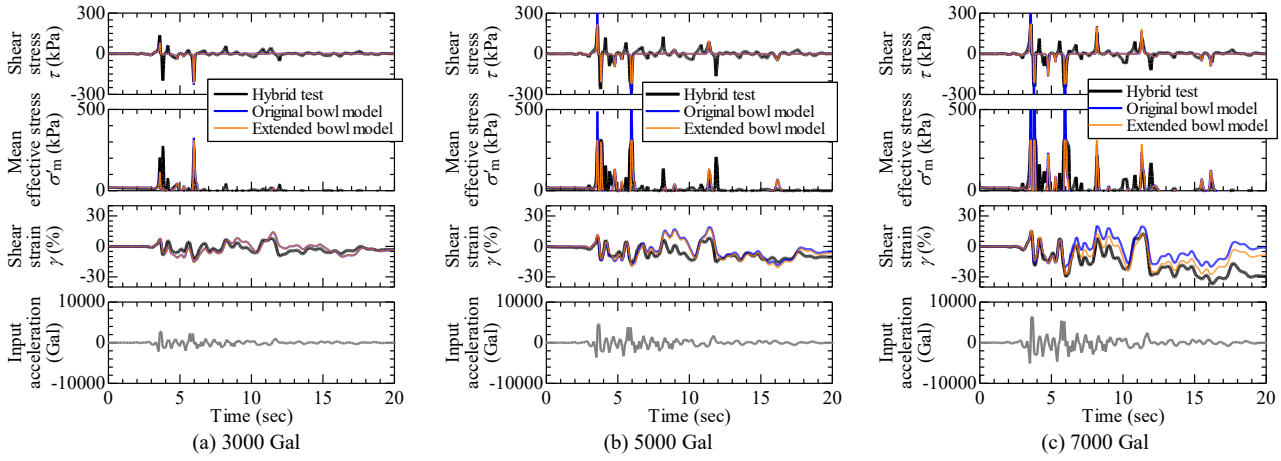

Figure 13. Time history of the responses at the tested / effective stress analysis layer

layer. In the original bowl model, excessive shear stress developed in the target layer, which led to increased acceleration in shallower layers and a reduction in displacement. In contrast, the effective stress analysis using the extended bowl model closely reproduced the test results. For the 5,000 Gal input, both the maximum shear stress and the vertical distribution of the acceleration response were almost identical to the experimental results. For 7,000 Gal input, although slight discrepancies were observed, the vertical distribution predicted by the extended bowl model was still closer to the test data than those predicted from the original bowl model. These findings indicate that the differences between the original and extended bowl models become more pronounced with increasing seismic intensity. Therefore,

accounting for the steady state using the extended bowl model is especially important when modeling response to extremely large earthquakes.

Fig. 12 shows the $\tau \sim \gamma$ relationships and $\sigma'_m \sim \gamma$ relationships of the target layer. For the 3,000 Gal input, the test result did not reach a steady state, indicating that the stress level was not high enough to induce such a condition. Consequently, similar results were obtained regardless of the analysis model.

In contrast, for the 5,000 and 7,000Gal inputs, the original bowl model predicted unbounded increase in both the shear stress and the mean effective stress, which deviated significantly from the experimental results On the other hand, the extended bowl model successfully reproduced the plateauing behavior observed in the test, with shear stress leveling off at about 220 kPa and mean effective stress at around 320 kPa. Furthermore, the extended bowl model accurately captured the trend of the shear strain development, whereas the original bowl model tended to underestimate it, particularly under the 7,000 Gal input condition.

Fig. 13 shows the time histories of shear stress, mean effective stress, shear strain of the test layer, and the input motion. For the 3000Gal input, both the original and the extended bowl models produced nearly identical responses. However, for the 5,000 and 7,000 Gal inputs, notable differences appear in the response of shear stress and mean effective stress around 4 and 6 seconds, when the input motion becomes large. The original bowl model overestimated the stress level, while the extended bowl model successfully captured the steady state behavior observed in the hybrid test. In particular, under the 7,000 Gal input, there is a significant discrepancy in the shear strain response. The extended bowl model, which accurately reproduce the steady state, showed results that closely matched the strain behavior observed in the hybrid ground response tests.

3.3 *Applicability of the extended bowl model*

The results of the reproducing analysis indicate that the extended bowl model, which incorporates the steady state, is effective for calculating stress conditions and acceleration response against L2 level or larger earthquake motions. Furthermore, depending on the condition of the liquefiable layer or surrounding ground layers, even smaller earthquakes can induce steady state phenomenon. In such cases, effective stress analysis using the extended bowl model may also be necessary. However, the model did not accurately reproduce the shape of the hysteresis curve or the strain development in small-strain range, particularly in the 3,000 Gal case. To improve the accuracy in this range, further refinement of the model and calibration of its parameters are required and remain important future research tasks.

4 CONCLUSIONS

In this study, an effective stress analysis model, termed the "extended bowl model" was developed to evaluate ground response under extremely large earthquakes by incorporating the steady state behavior of sandy soils. The concept of a critical void ratio e_{cr}, or critical effective stress σ'_{cr} under undrained conditions, was introduced into the bowl model. When the soil reaches these values, the "bowl" to consider pore water pressure shifts parallelly, enabling the model to represent steady state behavior.

Subsequently, reproduction analyses of hybrid ground response tests were conducted using the extended bowl model combined with the GHE model. The target layer consisted of Toyoura sand with a relative density of 60%, for which parameter fitting and effective stress analyses were performed. The results confirmed that the extended bowl model could accurately reproduce the results of the hybrid ground response tests, including the observed steady state behavior. Compared to the original bowl model which does not account for steady state conditions, the extended model provided improved predictions of critical response parameters such as shear stress, effective stress in the target layer, maximum acceleration, and displacement response at the ground surface which are key factors in the seismic design.

In the effective stress analysis, input motions up to 7,000 Gal were used to induce steady state phenomena in Toyoura sand and to verify the model and its parameters. The results demonstrate that the extended bowl model is effective for evaluating seismic ground response to L2 earthquake motions, particularly in areas where extremely strong shaking is expected, or the earthquake motion in the crisis resistance category. However, it should be noted that the shape of the hysteresis curve and the strain development at small strain levels were not fully reproduced with high accuracy. Therefore, further improvement of the model and refinement of parameter calibration remain as future research issues.

5 ACKNOWLEDGEMENTS

The authors would like to express their sincere gratitude to Mr. Mabuchi, S. and Mr. Kodama, T. of Itochu Techno-Solutions Corporation for their contributions in implementing the analysis model into a practical computational program. Their contributions greatly facilitated the numerical simulations conducted in this study.

6 REFERENCES

Fukushima, Y. and Midorikawa, S., 1994. Evaluation of average Q-1 value of surface soils and ground amplification factor based on frequency dependence, *The Architectural Institute of Japan's Journal of Structural and Construction Engineering* 460, 37-46. (In Japanese)

Fukutake, K. and Matsuoka, H., 1989. A unified law for dilatancy under multi-dimentional simple shearing. *Japanese Journal of JSCE*, 412/III-12. (in Japanese)

Fukutake, K., Ohtsuki, A., Sato, M., Shamoto, Y., 1990. Analysis of saturated dense sand-structure system and comparison with results from shaking table test. *Earthquake Engineering Strucucture Dynamics* 19(7), 977–992.

Fukutake, K. and Kiriyama, T., 2018. LEAP-2017 Centrifuge Test Simulation using HiPER, Model Tests and Numerical Simulations of Liquefaction and Lateral Spreading, Springer, 461-479.

Izawa, J., Toyooka, A., Kojima, K., Murono, Y., and Suzuki, A., 2019. Deformation properties of soils for a nonlinear dynamic response analysis, *Proc. the 7th International Conference on Earthquake Geotechnical Engineering*.

Nogami, Y., Murono, Y., Morikawa, H., 2012. Nonlinear hysterisis model taking into account S-shaped hysterisis loop and its standard parameters, *Proc. 15th World Conference on Earthquake Engineering*.

Railway Technical Research Institute, 2012. Design Standard for Railway Structure and Commentary (Seismic Design): Maruzen. (In Japanese)

Tatsuoka, F. and Shibuya, S., 1992. Deformation characteristics of soils and rocks form field and laboratory tests, Theme Lecture 1, *Proc. of Ninth Asian Regional Conference on Soil Mechanics and Foundation Engineering* Vol. 2, 101-170.

Verdugo, R. and Ishihara, K., 1996. The steady state of sandy soils, *Soils and Foundations* 36(2), 81-91.

Yamamoto, M., Ibuki, R., Yamauchi, Y., Kanzawa, T., and Izawa, J., 2022. Fundamental study on laboratory test method for setting parameters of effective stress analysis, *Proc. the 4th International Conference on Performance Based Design in Earthquake Geotechnical Engeneering*.

Yoshimine, M. and Ishihara, K., 1998. Flow potential of sand during liquefaction, *Soils and Foundations* 38(3), 189-198.